VPS VIBRATIONS IN PHYSICAL SYSTEMS

DOI: 10.21008/j.0860-6897.2024.1.20
Vibrations in Physical Systems, 2024, 35(1), 2024120

The effectiveness of damping for SkyHook control strategy depending on how realistic damper model is

Zbyszko KLOCKIEWICZ, **Grzegorz ŚLASKI**

Poznan University of Technology, Piotrowo 3, 60-965 Poznań

Corresponding author: Zbyszko KLOCKIEWICZ, email: zbyszko.klockiewicz@put.poznan.pl

Abstract One of the most widely known control strategies for improving vehicle ride comfort is SkyHook, which was tested by many scientists. Those tests however were carried out mainly using simplified damper models with simple linear or two-linear, symmetric characteristics. On the base of real damper characteristics testing, the researchers in this article examined the influence of using more realistic and complicated damper models with friction, hysteresis and time-delay of state-switching implemented, on the effectiveness of control goals. They were measured by chosen dynamic responses of a suspension system for excitations in the typical exploitation frequency range. The results from the experiments were compared with those found in literature and with the simplified version of a damper model, without hysteresis, friction or actuation delay.

Keywords: damping control strategy, SkyHook, adjustable damping, vehicle vertical dynamics, ride comfort, damper model, friction, hysteresis, actuation delay.

1. Introduction

The basic tasks of a suspension system is to ensure safe interactions between vehicle wheels and the road surface, while providing satisfactory ride comfort and working in a designated motion range. Oftentimes, satisfying all those needs at once proves impossible [1], as different parameters of suspension components have different optimal values for safety and comfort criteria and for different excitations and vehicle mass parameters changing with the varying vehicle load. Furthermore, the use of a damper in a typical configuration between sprung and unsprung masses in some mass motion cases helps to dampen vibrations, while inducing them in others. The need to change the way in which a damper works in different situations lead to the creation of suspension with dampers controlled by adaptive or semi-active control strategies. They allow to change some parameters or to switch the damping force during one cycle of vibration. The idea of such control is not new – the patent for adjustable hydraulic shock absorbers was granted in 1957 [2], while control strategies for computer models of vehicles were studied as far back as the 1980s [3]. The first widely spread control was introduced in 1973 comfort oriented SkyHook strategy [4], which since then was implemented numerous times in simulations and real-life applications [5-7]. Since then, many more control strategies have been proposed [8] including safety oriented GroundHook [9] and later Acceleration Driven Damper (ADD) [10, 11], Power Driven Damper (PDD) [11] or recently Energy Driven Damper (EDD) [12].

A lot of research work of SkyHook control strategy was done purely on theoretical, simplified vehicle models and the real-life implementation of said strategies, while not unseen, remains rare. The most often used simplified suspension models use simplified models of damping forces, often utilising linear damping coefficient and damping coefficient optimization is also frequently done using linear models [13]. More advanced damper models include nonlinear characteristics and/or asymmetrical characteristics [14], [15]. Those models have been gaining popularity, since in many cases foregoing their use introduces unacceptable levels of error [16]. Dry friction and force hysteresis, albeit rarely being implemented, is sometimes included in damping force calculations [6, 17]. The same is true for properties connected with damping force adjustment - especially the delay time between control signal and damping characteristic change [18].

The authors decided to research the influence of aforementioned additional features of the damper model on the effectiveness of the damping control strategy in comparison to the simple nonlinear model used as reference. The subject of research were changes in transfer functions of a quarter car model with different damper models (with internal friction, hysteresis and activation delay implemented) tested using a chirp signal with frequency range of 0.01 to 25 Hz. Analysis of these functions allowed to evaluate how big the difference in chosen dynamic responses is when using more advanced (and realistic) damper model in simulations – one with internal friction, hysteresis and activation delay implemented.

2. Research method

The research was made with the use of computer simulation of a set of quarter car vertical dynamics models implemented in Matlab/Simulink software. In each research case models build with different damper models presented in the Table 1 were simulated and their responses were compared with base model and analysed.

Case number 1 was chosen as a reference for changes observed for cases 2 to 5. It was the model with a static and asymmetrical damper characteristic acquired experimentally from real-life object. Other parameters of a suspension model (Table 2) were shared between all versions of a model – linear stiffness characteristics of a tire and suspension were used.

Table 1. Parameters of a quarter-car models tested during the research.

Case no.	Nonlinear characteristic	Friction	Hysteresis	Delay
1	✓	–	–	–
2	✓	✓	–	–
3	✓	–	✓	–
4	✓	–	–	✓
5	✓	✓	✓	✓

Table 2. Shared parameters of a quarter-car model.

Parameter	Unsprung mass [kg]	Sprung mass [kg]	Tire stiffness [kN/m]	Tire damping [Ns/m]	Suspension stiffness [kN/m]
Value	50	400	200	350	30

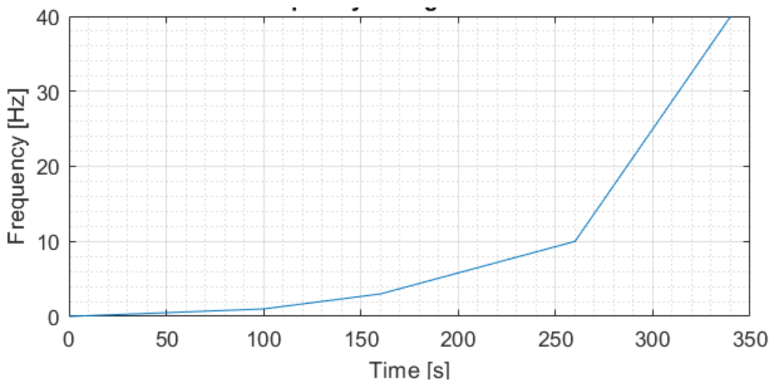

Figure 1. Changes of the frequency of the input signal over simulation time (340 s).

Models tested during simulation were subjected to the excitation enabling calculations of dynamic responses of the suspension in the form of transfer functions between excitation and responses important to evaluation of suspension dynamic performance. Following responses were chosen:

- suspension deflection for evaluation of necessary rattle space,
- sprung mass acceleration for evaluation of ride comfort,
- cumulative tire force for evaluation of safety potential.

The excitation used was a vertical sinusoidal displacement with a constant amplitude of 3 mm, that had variable frequency – starting from 0.0001 Hz up to 40 Hz (Fig. 1). The frequency values changed in a nonlinear fashion in order to allow more cycles in lower range to occur, which in turn gives better results when calculating transfer functions [16]. Frequencies, both below 0.5 and above 25 Hz, were added to the simulation in order to further stabilize results of the Matlab's *tfestimate* function used to estimate transfer functions of dynamic responses of the suspension.

2.1. Advanced adjustable damper model

The main model module is the base damper model – static damping characteristics module, modelling damping force as a function of deflection speed, differing for the compression and rebound and also dependent on the control current. An interpolation of experimental characteristics was used as a way of modelling damping forces and implemented in a Matlab/Simulink software via the Look up table [15]. For the adjustable damper the interpolation is also necessary for the value of damping force in relation to the control current. It required 2-dimensional Look up table block for the three dimensional shock absorber characteristics. Medium static damping characteristics was chosen as the base characteristic, its values between the forces registered for the lowest and highest control current. This characteristics was then multiplied by a specific number dependent on the control current and whether the damper was being compressed or extended, resulting in a force that is within range defined by maximum non-linear and minimum non-linear characteristics (see Fig. 2).

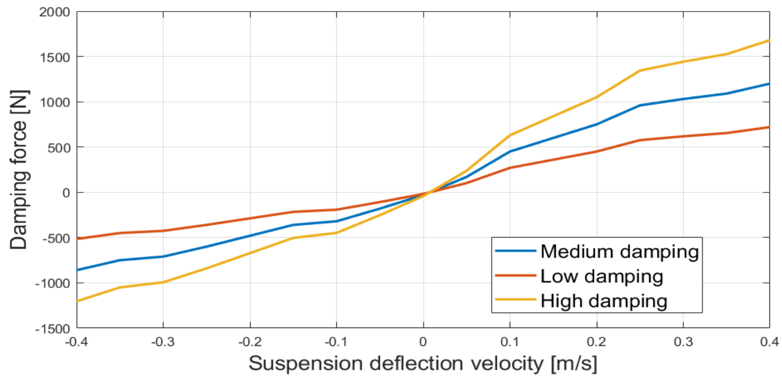

Figure 2. Damper model static characteristics.

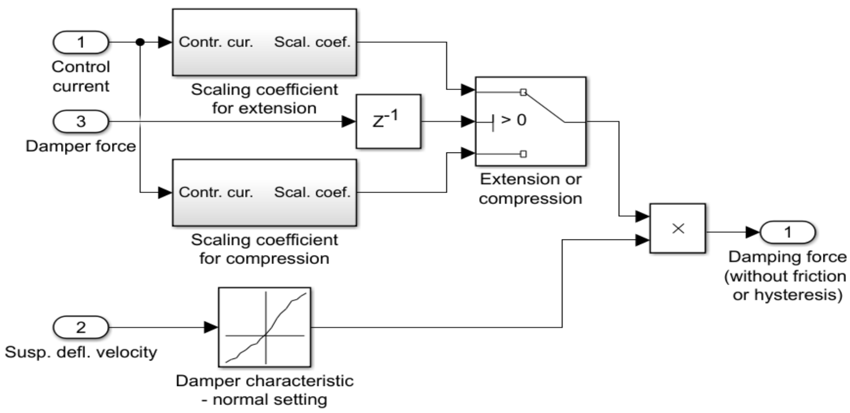

Figure 3. Damping force calculation subsystem.

The medium damping F_{ds_m} static characteristic was then modelled by the following formula:

$$F_{ds\_I} = F_{ds\_m} \cdot K_I \,, \tag{1}$$

where:

F_{ds_I} – interpolated value of damping force from static characteristic for a given control current,
F_{ds_m} – the middle static characteristics damping force (for middle value of valve coil current),
K_I – the coefficient to increase or decrease damping force in accordance to the value of valve coil current and the state of damper work – compression or rebound.

For the modelled shock absorber formulas for calculating K_I values according to current value I_c ($0.6 \leq I_c \leq 1.6$ [A]) were determined for compression and rebound respectively as:

$$K_{IC} = -0.55 I_c + 1.59 \quad \text{and} \quad K_{IR} = -0.71 I_c + 1.74. \tag{2}$$

The Simulink implementation of implementation of equations (1) and (2) is presented in Figure 3.

All more realistic versions of a damper model (cases no. 2 through 5) included additionally models of hysteresis, friction and actuation delay. These models were switched off individually for particular test cases. The implementation of this model, based on [7] was described in [18] and is shown in Figure 4. Three main modules to model the total damper force were applied:

- the static damping force,
- hysteresis force,
- friction force.

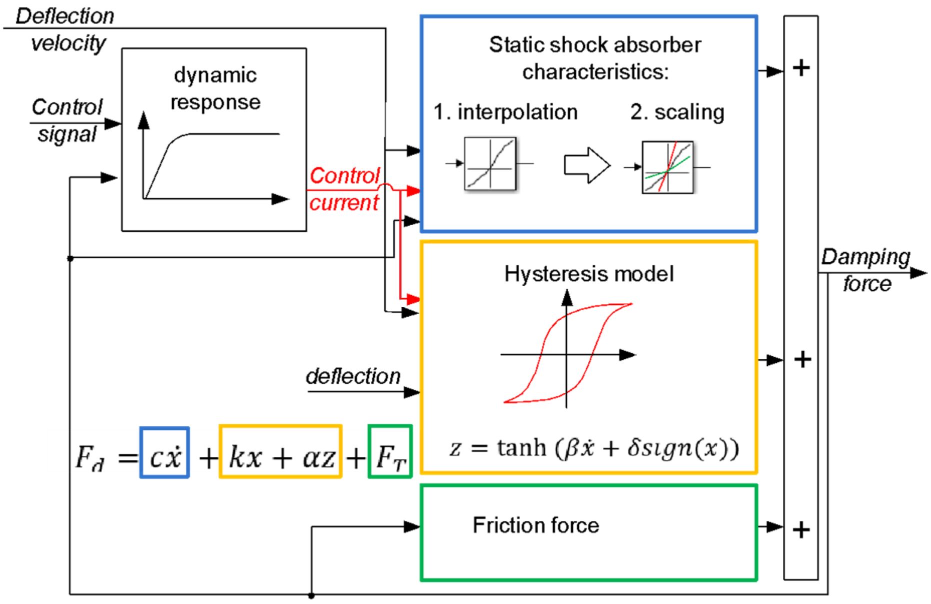

Figure 4. Damper model schematic [14].

The damper hysteresis module is important for high damping forces and high velocities. Simple model based on a work [6] is proposed to model the hysteretic force–velocity characteristic of the damper. This model is given by formulas:

$$F_h = kx + \alpha z, \tag{3}$$

$$z = F_0 \cdot \tanh\left(\beta\dot{x} + \delta \mathrm{sign}(x)\right), \tag{4}$$

where:

k – stiffness coefficient which is responsible for the hysteresis opening found from the vicinity of zero velocity; a large value of k corresponds to the hysteresis opening of the ends,

z – the hysteretic variable given by the hyperbolic tangent function,

β – the scale factor of the damper velocity defining the hysteretic slope; the large value of β gives a step hysteretic slope,

δ – factor determining the width of the hysteresis through the term δsign(x), a wide hysteresis is resulting from a large value of δ,

α – scale factor of the hysteresis that determines the height of the hysteresis; its value depends on the control current.

On the base of the analysis of dynamic characteristic of tested real shock absorber [15], a formula for the relation between scale factor α and valve coil current I_C was established as:

$$\alpha = \alpha_0 \cdot (-2.15 I_C + 4.45), \tag{5}$$

where α_0 – scale factor α of the hysteresis for middle static characteristics damping force.

Hysteresis force's value was dependent on both the suspension deflection and its velocity, as well as on the control current's value and a number of empirically obtained parameters [18].

The internal friction module models the force F_T and consists of two elements – the value of kinetic friction force and the signum function due to model friction force being opposite sign to the damping force. The friction force calculation depends on a suspension deflection velocity – if it is greater than a given threshold value of 0.1 m/s, the friction force has a value equal to the defined kinematic friction (35 N), if it is smaller – the kinematic friction value is multiplied by a ratio of current suspension deflection velocity to the threshold value (see Fig. 5):

$$F_f = \begin{cases} 35 & \text{if} \quad v_{defl} > 0.1 \text{ m/s} \\ 35 \cdot \frac{v_{defl}}{0.1} & \text{if} \quad v_{defl} < 0.1 \text{ m/s} \end{cases} \quad [N] \tag{6}$$

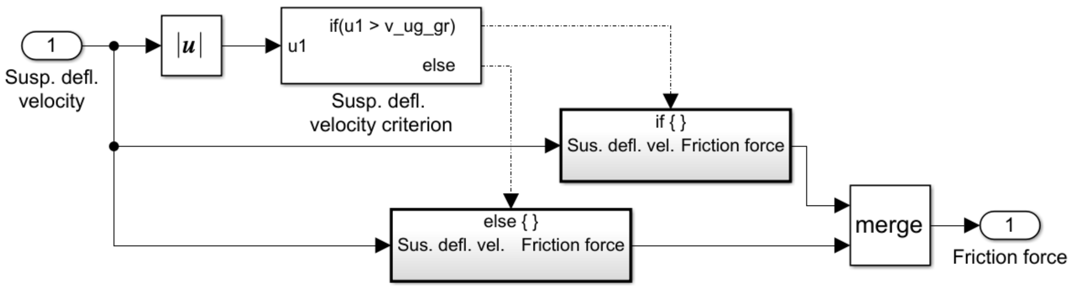

Figure 5. Friction force calculation subsystem.

The module modelling response time of a shock absorber is based on the model presented in [7, 15] and consists of two blocks modelling the delay for the damping force increase:

- dead time T_0,
- time delay with time constant T_Z.

Considering that the time response of tested shock absorbers depends on the stroke direction movement and on the valve operating state, including switching direction (from soft to hard or vice versa), the four different time delays using different values of T_0 and T_Z are calculated in the model and appropriate one is used according to compression/rebound movement and switching direction. For tested shock absorber these values were determined to be the same for compression and rebound directions and for switching from soft to hard. Those values are $T_0 = 4$ ms and $T_Z = 5$ ms and for switching from hard to soft: $T_0 = 2$ ms and $T_Z = 3$ ms.

Usage of more realistic models allowed to achieve the goals of the research, which was to check qualitative and quantitative influence of taking into account friction, hysteresis and delay time on the transfer function obtained for comfort oriented SkyHook control strategy.

All the versions of the model that had a control strategy implemented also had a delay module, which caused the current change to occur over a given amount of time. Those three modules – friction, hysteresis and delay – could be turned on or off to test their impact on the models behaviour.

3. Testing and methodology of analysis simulation results

In the experiments, a quarter car model containing a nonlinear damper model with controllable friction and hysteresis modules was used, those modules having option to be turned on or off. Besides damper module, the rest of the model was linear, with the parameters of the model presented in Table 2. For each variant the same excitation was applied – a changing frequency sine wave of amplitude 3 mm, with the course of frequency's variability shown in Figure 1.

The influence of implementing friction, hysteresis actuation delay and all those factors simultaneously was analysed for three indicators – suspension deflections, cumulative force between the tire and the road surface and sprung mass accelerations. Analysed indicators allowed for the suspension performance evaluation in terms of ride comfort, ride safety as well as kinematic limitations caused by the finite work range of the suspension.

Because those indicators are not defined by single value, but rather as a function of frequency, the tool chosen for the analysis were the transfer functions between given indicator and kinematic excitation. These functions were calculated using the response signals (deflection, cumulative tire force and sprung mass acceleration) obtained during simulations, to mimic what would be done for a real-life experiments. The transfer functions between those responses and kinematic excitation were then calculated in Matlab using *tfestimate* function for the nonlinear, passive model without friction, hysteresis and actuation delay modules, which served as a reference, to which results for other variants were then compared to. The reason why those functions were not calculated based on the element characteristics was the nonlinear character of control strategies and the damper itself. The resulting transfer functions were then plotted as graphs, showing their magnitude as the function of frequency, with the range of frequencies from 0.5 to 25 Hz being investigated.

The results for the relative values between a given case and the reference model were shown using bar charts for four chosen frequencies – near first resonant frequency (ca. 1 Hz), 3 Hz, second resonant frequency (around 10 Hz) and for maximum tested frequency 25 Hz.

4. Results

The influence of friction and hysteresis on transfer functions for SkyHook controlled suspension is similar to such influence on passive suspension – they act like the increase in damping force, causing the magnitudes for road excitation to suspension deflection transfer function to decrease (see Fig. 6).

Table 3 and Figure 6 present absolute and relative values of transfer functions of suspension deflection for damper model with SkyHook control strategy. Suspension deflections were mostly influenced by hysteresis for sprung mass resonant frequency and delay in actuation for unsprung mass resonant frequency.

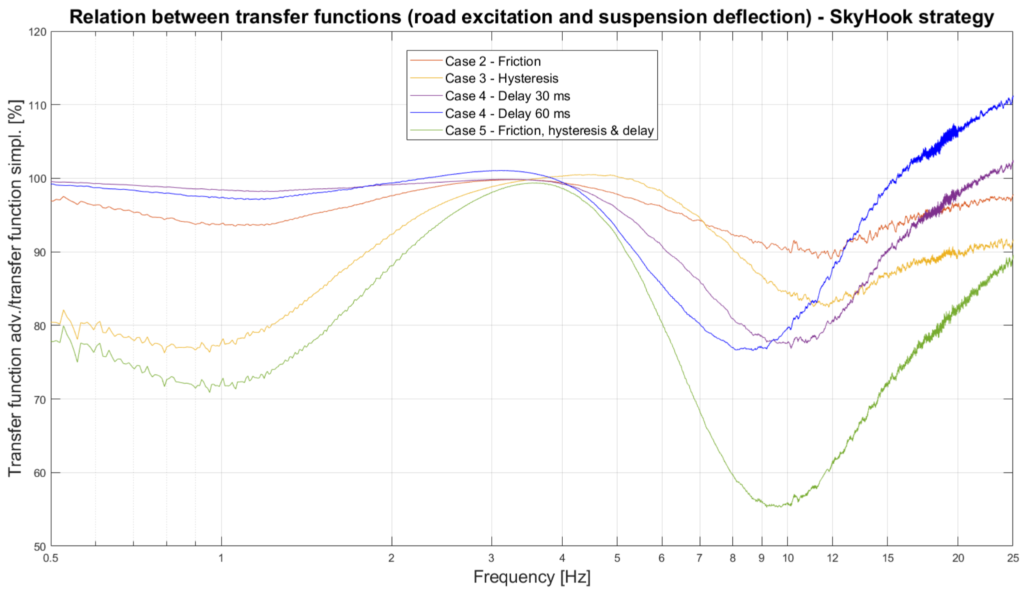

Figure 6. The influence of how realistic damper model is on suspension deflection transfer functions.

Table 3. Absolute values of transfer functions between road excitation and suspension deflection [m/m] for SkyHook.

	1st resonant freq. ~1 Hz	~3 Hz	2nd resonant freq. ~10 Hz	Max. tested freq. 25 Hz
Reference	0.82	1.08	1.15	0.18
Friction	0.77	1.08	1.01	0.18
Hysteresis	0.65	1.07	0.96	0.16
Delay 60 ms	0.80	1.08	0.87	0.19
Fric. + Hyst. + Delay 60 ms	0.60	1.06	0.63	0.16

 DOI: 10.21008/j.0860-6897.2024.1.20

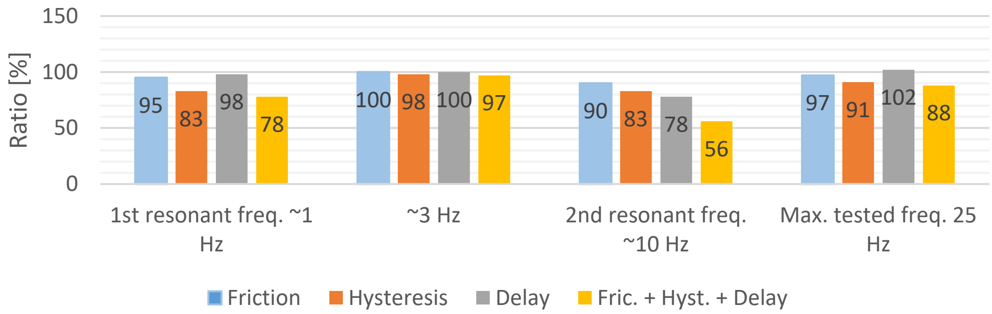

Figure 7. Relative values of suspension deflection transfer functions values for selected frequencies for SkyHook controlled suspension.

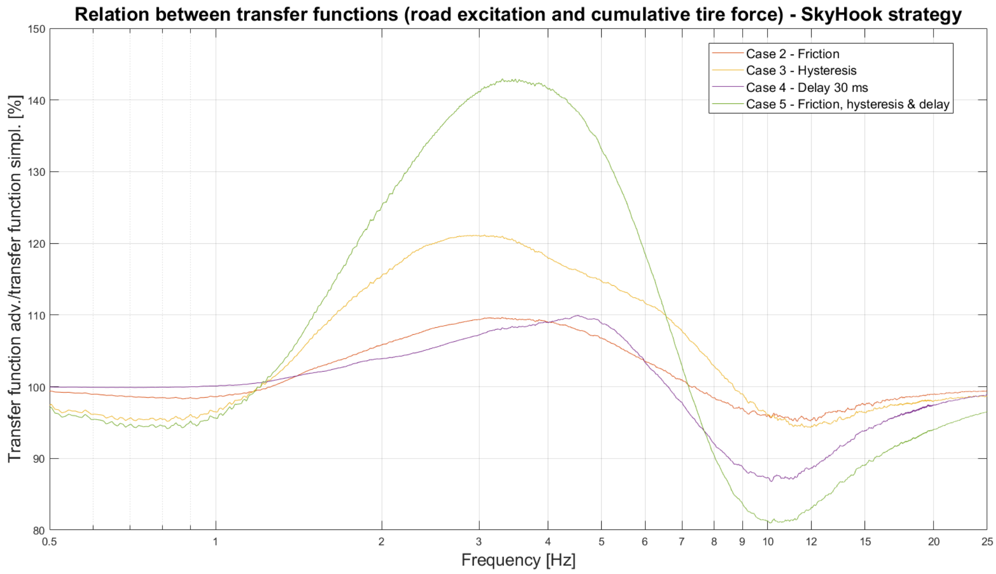

Figure 8. The influence of how realistic damper model is on cumulative tire force transfer functions.

Table 4. Absolute values of transfer functions between road excitation and cumulative tire force $\left[\frac{N\cdot 10^5}{m}\right]$ for SkyHook.

	1st resonant freq. ~1 Hz	~3 Hz	2nd resonant freq. ~10 Hz	Max. tested freq. 25 Hz
Reference	0.36	0.82	3.05	2.39
Friction	0.37	0.90	2.85	2.38
Hysteresis	0.37	1.03	2.98	2.37
Delay 60 ms	0.37	0.88	2.65	2.37
Fric. + Hyst. + Delay 60 ms	0.37	1.20	2.53	2.30

Figure 8 presents changes in transfer functions comparing to case no 1. Table 4 and Figure 8 present absolute and relative values of transfer functions of cumulative tire force for damper model with SkyHook control strategy.

Cumulative tire forces were mostly influenced by hysteresis for 3 Hz and delay for 10 Hz (see Fig. 10). The biggest changes in general were seen for 3 Hz range, where implementation of all three advanced options to the damper model caused to transfer function value to increase by over 40% compared to the reference model, aside from that for other frequencies the change was no larger than 13%.

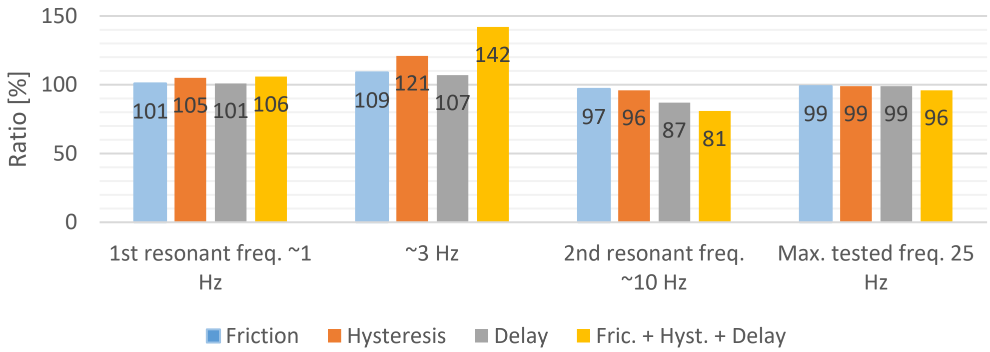

Figure 9. Relative values of cumulative tire force transfer functions values for selected frequencies for SkyHook controlled suspension.

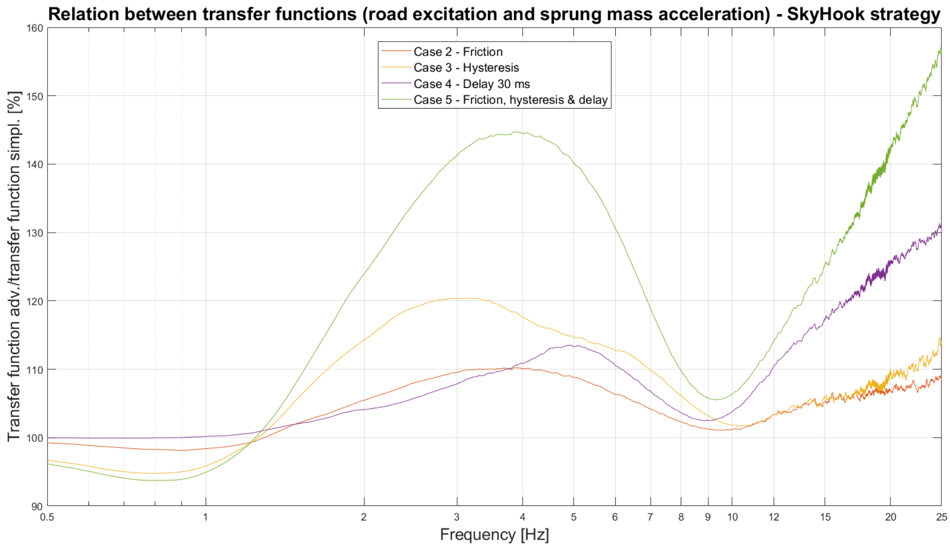

Figure 10. The influence of how realistic damper model is on cumulative tire force transfer functions.

Table 5. Absolute values of transfer functions between road excitation and sprung mass acceleration $\left[\frac{m}{s^2}/m\right]$ for SkyHook.

	1st resonant freq. ~1 Hz	~3 Hz	2nd resonant freq. ~10 Hz	Max. tested freq. 25 Hz
Reference	90	190	460	205
Friction	90	205	465	225
Hysteresis	90	230	475	235
Delay 60 ms	90	200	470	270
Fric. + Hyst. + Delay 60 ms	90	265	485	325

Table 5 and Figure 9 present absolute and relative values of transfer functions of sprung mass accelerations for damper model with SkyHook control strategy.

The influence on sprung mass accelerations of all three factors for both resonant frequencies was small, reaching 6% at most, however it could be much more clearly seen for 3 Hz and 25 Hz. As could be expected, the higher the frequency, to more important delay in actuation became – with it contributing to over 30% higher transfer function values.

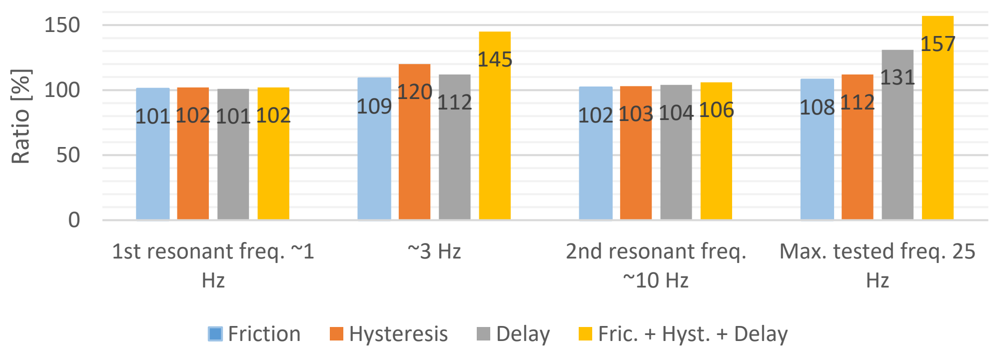

Figure 11. Relative values of sprung mass accelerations transfer functions values for selected frequencies for Sky Hook controlled suspension.

4. Conclusions

Obtained results proved that using more realistic shock absorber model, that includes friction, hysteresis and delay, mostly causes that model to act like having increased damping coefficient in simpler damper model. The exact influence depends on the frequency and which transfer function are analysed.

Suspension deflections were mostly influenced by hysteresis for sprung mass resonant frequency and delay in actuation for unsprung mass resonant frequency. Friction had a lesser impact on transfer function values overall. It can also be noted that all three factors combined caused a bigger difference in transfer function value than the sum of their individual influences.

The magnitude of transfer functions between road excitation and both cumulative tire force as well as sprung mass acceleration increases or stays almost the same (dropping by at most 5% in comparison to reference model). The increase is more significant for those functions than decrease was for suspension deflection – especially in the range of 3 to 4 Hz, where friction causes 10% increase and hysteresis contributes to 20% increase. Those values drop significantly being on par with reference model for cumulative tire force, while for sprung mass acceleration after going down to around 102–104% of reference value in the range of 9–10 Hz they increase again up to maximum tested frequency of 25 Hz.

Actuation delay makes little difference for low frequencies, but its influence starts growing once 1 Hz frequency is achieved, peaking around 3 Hz, when it starts to drop again. Delay of 30 ms did not have much of an impact on lower frequency response, as was expected. With the growing frequency, its influence rose, which could be observed for sprung mass accelerations and cumulative tire force as the relative increase in magnitude for frequencies in the range of 1.5 to 6 Hz. For suspension deflections, the changes become apparent around 4 Hz value, when relative magnitude starts dropping quickly, reaching 75% for 10 Hz, when it starts going back up, reaching 102% for 25 Hz. The drop in value is visible for other analysed data as well, along with the rise of relative magnitude for values over 10 Hz. Because of the nature of excitation, which is periodical, this behaviour is caused by the fact that the delayed response first starts to act in counterphase to the intended changes, but after reaching a certain threshold the change from a previous cycle starts to coincide with the next excitation cycle, making the strategy work better. This is supported by a test, in which 60 ms delay was added and the results for both 30 ms and 60 ms delays were plotted – it was noticed that for 60 ms the analogous changes were happening for lower frequencies. The effects of friction, hysteresis and delay combined once again added up to the total effect in the model with all three active.

Of course the level of observed influences could be the different if the levels of friction, hysteresis or delays were significantly higher or lower, but used values were based on real damper testing and thus results are close to real word case.

It is also clearly visible that including advanced damper modules (in effect – more realistic damper model) affects important suspension performance indicators in non-negligible ways for a number of frequencies.

Additional information

The authors declare: no competing financial interests and that all material taken from other sources (including their own published works) is clearly cited and that appropriate permits are obtained.

References

1. P.S. Els, N.J. Theron, P.E. Uys, M.J. Thoresson; The ride comfort vs. handling compromise for off-road vehicles; J. Terramechanics, 2007, 44(4), 303–317
2. C. Sturari; Adjustable shock absorber, US2780321, 1957
3. C. Yue; Control law designs for active suspensions in automotive vehicles; MSc thesis, Massachusetts Institute of Technology, 1988
4. M.J. Crosby, D.C. Karnopp; The Active Damper – A New Concept for Shock and Vibration Control; Shock Vib. Bull., 1973, 43, 119–133
5. J. Emura, S. Kakizaki, F. Yamaoka, M. Nakamura; Development of the Semi-Active Suspension System Based on the Sky-Hook Damper Theory; J. Passeng. Cars, 1994, 103, 1110–1119
6. K.-S. Hong, H.-C. Sohn, J. K. Hedrick; Modified Skyhook Control of Semi-Active Suspensions: A New Model, Gain Scheduling, and Hardware-in-the-Loop Tuning; J. Dyn. Syst. Meas. Control, 2002, 124(1), 158–167
7. S.M. Savaresi, C. Spelta; Mixed Sky-Hook and ADD: Approaching the Filtering Limits of a Semi-Active Suspension; J. Dyn. Syst. Meas. Control, 2007, 129(4), 382–392
8. G. Ślaski; Studium projektowania zawieszeń samochodowych o zmiennym tłumieniu; Wydawnictwo Politechniki Poznańskiej, 2012
9. M. Valášek, M. Novák, Z. Šika, O. Vaculín; Extended ground-hook - New concept of semi-active control of truck's suspension; Veh. Syst. Dyn., 1997, 27(5–6), 289–303
10. S.M. Savaresi, E. Silani, S. Bittanti; Acceleration-Driven-Damper (ADD): An Optimal Control Algorithm For Comfort-Oriented Semiactive Suspensions; J. Dyn. Syst. Meas. Control, 2005, 127(2), 218–229
11. S.M. Savaresi, C. Poussot-Vassal, C. Spelta, O. Sename, L. Dugard; Semi-Active Suspension Control Design for Vehicles, 2010
12. H. Gao, Z. Li, W. Sun; Energy-Driven-Damper (EDD): Comfort-Oriented Semiactive Suspensions Optimized From an Energy Perspective; IEEE Trans. Control Syst. Technol., 2020, 28(5), 2069–2076
13. Z. Lozia; The use of a linear quarter-car model to optimize the damping in a passive automotive suspension system – a follow-on from many authors' works of the recent 40 years; Arch. Automot. Eng. (Arch. Motoryzacji), 2016, 71(1), 39–72
14. B.A. Abebe, J. Santhosh, A.A. Ahmed, P. Murugan, N. Ashok; Non-Linear Mathematical Modelling for Quarter Car Suspension Model; Int. J. Emerg. Technol., 2020, 11(5), 536–544
15. P. Zdanowicz, Z. Lozia; Wyznaczenie optymalnej wartości współczynnika asymetrii amortyzatora pasywnego zawieszenia samochodu z wykorzystaniem modelu „ćwiartki samochodu"; Pr. Nauk. Politech. Warsz. Transp., 2017, 119, 249–265
16. Z. Klockiewicz, G. Ślaski, M. Spadło; The Influence of the Conditions of Use and the Type of Model Used on the Vertical Dynamic Responses of a Car Suspension; Arch. Automot. Eng. (Arch. Motoryzacji), 2019, 85(3), 57–82
17. D. Więckowski, K. Dąbrowski, G. Ślaski; Adjustable shock absorber characteristics testing and modelling; IOP Conf. Ser. Mater. Sci. Eng., 2018, 421, 022039
18. K. Dąbrowski; Algorytmizacja adaptacyjnego sterowania tłumieniem zawieszenia samochodu dla uwzględnienia zmienności warunków eksploatacji; PhD thesis, Poznan University of Technology, 2018